DMD Fast Forward. Published on October 26, 2011 as doi:10.1124/dmd.111.042861

DMD #42861

Characterization of Aldehyde Oxidase Enzyme Activity in Cryopreserved Human Hepatocytes

J. Matthew Hutzler, Young-Sun Yang, Daniel Albaugh, Cody L. Fullenwider,

Jennifer Schmenk, and Michael B. Fisher

Translational Research (DMPK)

Boehringer-Ingelheim Pharmaceuticals Inc.

Ridgefield, CT

DMD Fast Forward. Published on October 26, 2011 as DOI: 10.1124/dmd.111.042861
This article has not been copyedited and formatted. The final version may differ from this version.

Running Title: Aldehyde Oxidase Activity in Cryopreserved Hepatocytes

*Address Correspondence to:

Dr. J. Matthew Hutzler

Boehringer-Ingelheim Pharmaceuticals Inc., Translational Research (DMPK)

175 Briar Ridge Road, R&D 10578, Ridgefield, CT 06877

Tel: 203-791-5978

Fax: 203-791-6130

Email: Matt.Hutzler@Boehringer-Ingelheim.com

Text Pages: 35

Tables: 1

Figures: 5

References: 32

Words in Abstract: 233

Words in Introduction: 612

Words in Discussion: 1625

Non-Standard Abbreviations:

AO, aldehyde oxidase; XO, xanthine oxidase; IVIVC, in vitro-in vivo correlation; P450, cytochrome P450; Cl_{int}, intrinsic clearance; Cl_h, hepatic clearance; HLM, human liver microsomes; Q_h, liver blood flow

DMD Fast Forward. Published on October 26, 2011 as DOI: 10.1124/dmd.111.042861
This article has not been copyedited and formatted. The final version may differ from this version.

Abstract

Substrates of aldehyde oxidase (AO) for which human clinical pharmacokinetics are reported were selected and evaluated in pooled mixed-gender cryopreserved human hepatocytes in effort to quantitatively characterize AO activity. Estimated hepatic clearance (Cl_h) for BIBX1382, carbazeran, O^6-benzylguanine, zaleplon, and XK-469 using cryopreserved hepatocytes was 18, 17, 12, <4.3, and <4.3 mL/min/kg, respectively. The observed metabolic clearance in cryopreserved hepatocytes was confirmed to be a result of AO-mediated metabolism via two approaches. Metabolite identification following incubations in the presence of $H_2{}^{18}O$ confirmed that the predominant oxidative metabolite was generated by AO, as expected isotope patterns in mass spectra were observed following analysis by high resolution (LTQ-Orbitrap) mass spectrometry. Secondly, clearance values were efficiently attenuated upon co-incubation with hydralazine, an inhibitor of AO. The low exposure following oral doses of BIBX1382 and carbazeran (~5% F) would have been fairly well predicted using simple hepatic extraction (f_h) values derived from cryopreserved hepatocytes. In addition, the estimated hepatic clearance value for O^6-benzylguanine was within ~80% of the observed total clearance in humans following IV administration (15 mL/min/kg), indicating a reasonable level of quantitative activity from this in vitro system. However, a 3.5-fold under-prediction of total clearance was observed for zaleplon, despite the 5-oxo metabolite being clearly observed. Collectively, data suggests that the use of cryopreserved hepatocytes may be a practical approach for assessing AO-mediated metabolism in discovery, and potentially useful for predicting hepatic clearance of AO substrates.

DMD Fast Forward. Published on October 26, 2011 as DOI: 10.1124/dmd.111.042861
This article has not been copyedited and formatted. The final version may differ from this version.

Introduction

Aldehyde oxidase (AO) belongs to a family of enzymes referred to as molybdenum cofactor-containing enzymes that also includes xanthine oxidase (XO). This drug-metabolizing enzyme is active as a homo-dimer composed of two identical ~150 kDa subunits and demonstrates broad substrate selectivity, oxidizing a variety of aldehydes and heterocyclic-containing drug molecules (Beedham, 1987; Kitamura et al., 2006; Garattini et al., 2008). Of the known substrates of AO, it is heterocyclic ring-containing molecules that are of highest interest, as medicinal chemists commonly introduce these particular ring systems into chemical scaffolds in an effort to optimize towards improved solubility and lower lipophilicity, which in general, also yields reduced metabolism by cytochrome P450 enzymes. This chemistry strategy, while generally successful, may ultimately lead to alternative metabolic clearance mechanisms such as those catalyzed by AO.

Aldehyde oxidase has numerous features that make studying this enzyme challenging in a preclinical setting. Firstly, AO is present in the cytosolic fraction, and thus, standard metabolic stability studies using liver microsomes do not capture AO-mediated metabolism. If one is not cautious, then this metabolic pathway could be, and in fact has been, completely over-looked (*vida infra*). Additional intricacies of this enzyme include apparent donor-to-donor variability in activity in humans (Al-Salmy, 2001; Sahi et al., 2008), as well as across pre-clinical species and strains, where rats generally have low activity, and dogs are completely devoid of activity (Beedham et al., 1987; Garattini et al., 2008). Interest in this drug-metabolizing enzyme by the pharmaceutical industry has recently increased (Pryde et al., 2010; Garattini and Terao, 2011), with the recognition that extensive AO metabolism has led to severe clinical implications, either due to toxicological outcomes (Diamond et al., 2010), or higher-than-predicted clearance in

humans (Kaye et al., 1984; Rosen et al., 1999; Dittrich et al., 2002; Zhang et al., 2011; Akabane et al., 2011), yielding unacceptable pharmacokinetic properties. In most of these cases, either metabolic pathways were only evaluated in liver microsomes, or predictions of human clearance were extrapolated from pre-clinical species that possessed significantly lower AO activity compared to humans.

Scaling in vitro metabolism data to predict metabolic clearance is a critical component for half-life estimation, and ultimately, efficacious dose projections for new chemical entities moving towards clinical development. Scaling of in vitro metabolism data is a common approach for drug molecules that are primarily metabolized and cleared by cytochrome P450-mediated metabolic pathways (Houston, 1994; Obach et al., 1997), with numerous examples of successful predictions (Obach, 2000; Hutzler et al., 2010). However, collectively, there is inadequate information about the ability to scale in vitro clearance for compounds that are substrates of AO using hepatocytes, and assessment of AO metabolic activity is not included in characterization sheets when hepatocytes are received from vendors. To our knowledge, only one study has evaluated the ability to scale in vitro AO metabolism data using cytosol and S-9 fraction (Zientek et al. 2010), and under-predictions of free intrinsic clearance were noted. In addition, questions persist about the reported instability of the AO enzyme (Duley et al., 1985; Al-Salmy, 2001), which calls into question whether AO activity in current in vitro systems often used for scaling (e.g. cryopreserved hepatocytes) is representative of the in vivo situation. It also seems plausible that different proprietary hepatocyte isolation procedures by vendors may compromise AO activity. In effort to address this current knowledge gap, the objective of this work was to evaluate and compare AO activity in cryopreserved hepatocytes from two different vendors using substrates that are reported to be primarily cleared by AO-mediated metabolism

(Figure 1), and for which human clinical pharmacokinetics have been reported. In vitro-in vivo correlations for AO activity following standard scaling approaches from cryopreserved hepatocytes are reported herein.

DMD Fast Forward. Published on October 26, 2011 as DOI: 10.1124/dmd.111.042861
This article has not been copyedited and formatted. The final version may differ from this version.

Materials and Methods

Chemicals. Potassium phosphate buffer, O^6-benzylguanine, XK-469, zaleplon, hydralazine, midazolam, propranolol, NADPH and ^{18}O-water (97% purity) were purchased from Sigma-Aldrich (St. Louis, MO). BIBX1382, BIBU1476, and carbazeran were acquired from the internal compound library at Boehringer-Ingelheim Pharmaceuticals (Ridgefield, CT). Pooled human intestinal cytosol was purchased from Celsis/In Vitro Technologies (Baltimore, MD) and cryopreserved human hepatocytes along with hepatocyte media and reagents were purchased from both Celsis/In Vitro Technologies (Baltimore, MD) and Life Technologies (Carlsbad, CA). All other reagents and chemicals were of the highest purity available.

Hepatocyte Incubations. Pooled mixed gender cryopreserved human hepatocytes were obtained from Celsis/In Vitro Technologies (lot number OOO, 19 donors) and Life Technologies (lot number HuE104, 10 donors) and stored in liquid nitrogen until use. Immediately prior to experiments, sufficient aliquots of hepatocytes were thawed rapidly (~2 min) in a shaking water bath at 37°C. The contents of each vial were diluted 1/50 in pre-warmed (37°C) cryopreserved hepatocytes recovery medium (CHRM, Life Technologies, lot HuE104) or Williams' Medium E (WME, lot OOO) (pH 7.4) and gently mixed prior to centrifugation at 100 x g for 6 min at room temperature. Following centrifugation, the supernatant was discarded and the hepatocyte pellet was re-suspended in WME to provide 1 x 10e^6 cells/mL by repeated gentle inversion in a capped tube, and the cell number and viability were determined using a hemocytometer after staining with trypan blue. Viabilities for each hepatocyte experiment were at least 80%. The cell suspension was diluted in WME to give two times the incubation concentration and pre-warmed at 37°C for 15 min. Solutions of substrates (10% acetonitrile in H_20) were diluted in pre-warmed WME (giving an incubation concentration of organic solvent ≤0.1%). Incubations (performed in

quadruplicate) were initiated by the addition of substrate solution (250 µl) to the hepatocyte suspension (250 µl, 250,000 viable cells) in a 48-well tissue culture treated polystyrene incubation plate (1 µM final substrate concentration), followed by gentle swirling in an atmosphere of 5% CO_2 and 95% relative humidity (37°C). Incubations in the presence of the AO inhibitor hydralazine (50 µM) were conducted the same as described above, with hydralazine stock solutions prepared in water (10 mM). Reactions were terminated at 0, 5, 15, 30, 60 and 120 min by aliquoting 50 µL of incubate into 150 µL of cold acetonitrile (0.1% acetic acid) containing internal standard (0.25 µM tolbutamide). Quench plates were then centrifuged at 3000 x g (4°C) for 5 min, and supernatants were transferred to clean 96 well plates for LC/MS/MS bioanalysis.

Metabolite Profiling in Hepatocytes. The metabolite profile of each AO substrate was also evaluated following incubation at 10 µM in cryopreserved human hepatocytes (Lot OOO). Preparation of hepatocytes was similar to procedures described for in vitro clearance experiments, except that 2.0 x $10e^6$ cells/mL was the final concentration for metabolite generation. For incubations in the presence of ^{18}O-water, substrate solutions were prepared in the ^{18}O-water (250 µL), and 250 µL of cell suspension was added to initiate incubation (50% v/v, final). Following 120 min incubation in 24-well culture plates, reactions were terminated by addition of two volumes of cold acetonitrile, and the resulting mixture underwent centrifugation at 3000 x g (4° C) for 10 min. The supernatants were then transferred to clean glass test tubes, and subsequently dried under a gentle stream of nitrogen (N_2) gas. Dried samples were then reconstituted in 200 µl of mobile phase (85:15 (v/v) water/acetonitrile (0.1% formic acid)) and centrifuged again at 13,000 x g for 10 min prior to bioanalysis by high resolution mass spectrometry.

DMD Fast Forward. Published on October 26, 2011 as DOI: 10.1124/dmd.111.042861
This article has not been copyedited and formatted. The final version may differ from this version.

Intestinal Cytosol Incubations. Metabolic stability of carbazeran, BIBX1382, zaleplon, XK-469, and O^6-benzylguanine was evaluated in human mixed gender (6 donors) intestinal cytosol in 96-well deep well assay plates. Incubations were conducted in 100 mM potassium phosphate pH 7.4 buffer and 1 mg/mL intestinal cytosol with a final incubation volume of 0.4 mL. Reactions were initiated by addition of test compounds (1 µM, final organic <0.1%). Aliquots (50 µL) were removed from the cytosol assay at 0, 5, 15, 30, 60 and 120 min, and added to 150 µL of cold acetonitrile containing tolbutamide as an internal standard. Quenched samples were then centrifuged at 3000 x g (4°C) for 10 min to precipitate proteins, and the supernatant was transferred to clean 96-well plates for LC/MS/MS bioanalysis.

Liquid Chromatography/Mass Spectrometry Analysis. Quantitation of all analytes was performed using an AB Sciex API-5000 triple quadrupole mass spectrometer equipped with electrospray ionization (ESI) interface in positive ion mode and connected in-line to a Waters Acquity UPLC® system. Separation of analytes was performed using a Waters Acquity BEH high-pressure C_{18} 1.7µm (2.1 x 50mm) column held at 50°C. Mobile phase was flowed at 0.5 mL/min with a rapid gradient starting at 95%A (0.1% formic acid in water) and 5%B (0.1% formic acid in acetonitrile), held for 0.5 min, then ramped linearly to 5:95 A:B, and held for 1.3 min, followed by returning to initial conditions (3 minutes total run time). The MRM transitions for each analyte were as follows: carbazeran (*m/z* 360.9>272.1), BIBX1382 (*m/z* 388.0>98.0), zaleplon (*m/z* 306.2>236.2), XK-469 (*m/z* 345.0>273.0), O^6-benzylguanine (*m/z* 242.0>199.1), and tolbutamide (*m/z* 271.3>91.1). Standard curves for each analyte were prepared with concentration range of 0.003-2.0 µM, with limit of quantitation (LOQ) of 0.008 µM. All data were analyzed using AB Sciex Analyst 1.4.2 software.

DMD Fast Forward. Published on October 26, 2011 as DOI: 10.1124/dmd.111.042861
This article has not been copyedited and formatted. The final version may differ from this version.

Metabolite profiling of in vitro samples following incubation with cryopreserved human hepatocytes was performed using a high resolution LTQ-Orbitrap XL (Thermo Scientific, Waltham, MA) mass spectrometer connected to a Thermo Accela UPLC pump and CTC PAL auto-sampler (Leap Technologies, Carrboro, NC). The Orbitrap was equipped with an electro-spray ionization (ESI) source in positive polarity, and was calibrated using ProteoMass LTQ/FT-Hybrid Calibration Mix (Supelco, Bellefonte, PA) for mass accuracies < 5 ppm in external calibration mode. The source voltage was set at 5 kV, tube lens voltage at 90 V, and capillary voltage at 5 V, with the capillary temperature at 325°C. Sheath gas flow was at 70 U, aux gas at 15 U, and sweep gas flow at 5. Analytes were loaded (20 µL injection) onto a SUPELCO Discovery C_{18} (5-µm, 2.1 x 150 mm; Supelco, Bellefonte, PA) column and separated using a gradient elution profile consisting of solvent A (0.1% formic acid in water) and solvent B (0.1% formic acid in acetonitrile). The gradient was initiated at an 95%A:5%B ratio at a flow rate of 0.4 mL/min, held for 5 min, then ramped linearly from 5% B to 48% B over 10 min, then to 95%B over the next minute, and held for 2 min. The gradient was then returned to initial conditions, and column was allowed to re-equilibrate for 3 min (total run time 22 min). The HPLC eluent was introduced first into a photodiode array detector (PDA) set at 254 nm, and subsequently via electrospray ionization directly into the Orbitrap. Mass spectrometry analyses were carried out utilizing full-scan MS with a mass range of 100-1000 Da and MS/MS spectra were collected in a data-dependent fashion with relative collision energies of 50 and 35% for HCD and CID, respectively. Resolution was set at 30000 for FT MS, and 15000 for FT MS/MS. All mass spectral data were analyzed using Xcalibur version 2.1 software, and chemical structures and calculated exact mass estimates for fragments were generated using ChemDraw Ultra Version 12 software (Cambridge, MA).

DMD Fast Forward. Published on October 26, 2011 as DOI: 10.1124/dmd.111.042861
This article has not been copyedited and formatted. The final version may differ from this version.

Hepatic Clearance Estimates. In vitro intrinsic clearance (Cl_{int}) was estimated from cryopreserved human hepatocytes using substrate depletion methodologies and Equation 1:

$$Cl_{int} = 0.693 \times \frac{1}{t_{1/2}} \times \frac{ml\ incubation}{hepatocytes} \times \frac{gm\ liver\ wt}{kg\ body\ wt} \times \frac{hepatocytes}{gm\ liver\ wt}$$

where $t_{1/2}$ is the observed in vitro substrate depletion half-life (min), and 25.7 gm liver weight per kg body weight, and 120 x 10e^6 hepatocytes per gram liver were used as scaling factors. Hepatic clearance (Cl_h) was predicted using Cl_{int} values and the well-stirred model according to Equation 2:

$$Cl_h = \frac{Q_h \times f_u \times Cl_{int}}{Q_h + (f_u \times Cl_{int})}$$

where Q_h is human hepatic blood flow (20.7 mL/min/kg), f_u is fraction unbound in plasma, and Cl_{int} is in vitro intrinsic clearance derived from in vitro experiments in hepatocytes. Hepatic extraction ratio (E_h) is a measure of the liver's ability to extract drug prior to reaching the systemic circulation, and can be estimated using Equation 3:

$$E_h = \frac{Cl_h}{Q_h}$$

where Cl_h is hepatic clearance estimated from in vitro metabolic stability data from cryopreserved hepatocytes, and Q_h is hepatic liver blood flow (20.7 mL/min/kg in human). Oral bioavailability may be estimated using Equation 4:

$$F = F_{abs} \times F_g \times F_h$$

where F_{abs} is the fraction of the dose that is absorbed from the intestinal lumen to the enterocytes, F_g is the fraction of the dose that escapes intestinal first-pass metabolism, and F_h is the fraction of the dose that passes through the liver without being metabolized, also estimated by 1-E_h. Assuming complete absorption (F_{abs} = 1), and limited intestinal metabolism (F_g = 1), oral

DMD Fast Forward. Published on October 26, 2011 as DOI: 10.1124/dmd.111.042861
This article has not been copyedited and formatted. The final version may differ from this version.

bioavailability would be comparable to F_h ($F \approx F_h$). Thus, oral bioavailability was estimated using the following relationship (Equation 5):

$$F = 1 - E_h$$

DMD Fast Forward. Published on October 26, 2011 as DOI: 10.1124/dmd.111.042861
This article has not been copyedited and formatted. The final version may differ from this version.

Results

Hepatocyte Intrinsic Clearance. BIBX1382, carbazeran, *O*^{6}-benzylguanine, zaleplon, and XK-469 were incubated in pooled mixed-gender cryopreserved human hepatocytes from two different vendors to estimate hepatic clearance and quantitatively evaluate AO activity by comparing to known human pharmacokinetic data (Table 1). Firstly, there appeared to be negligible differences in activity in the two lots of hepatocytes tested, as predicted hepatic clearance values (mL/min/kg) for each of the substrates tested were within 87% of each other. In addition, data among the four replicates displayed high consistency with low standard deviations (Table 1). BIBX1382 and carbazeran both displayed high predicted hepatic clearances of 17-18 mL/min/kg, which equates to 84-88% of human liver blood flow (20.7 mL/min/kg). This is consistent with what has been observed clinically in humans following intravenous and/or oral dosing (e.g. high clearance and low oral bioavailability). Hepatic clearance of *O*^{6}-benzylguanine ranged from 11.2 to 12.8 mL/min/kg in cryopreserved hepatocytes, which is 72-82% of the observed total clearance reported in humans (15.6 mL/min/kg). Zaleplon was a substrate for which low rates of metabolism were observed in intrinsic clearance studies (<4.3 mL/min/kg), despite the fact that it is a moderate to high clearance drug in humans with a reported total clearance of 15.7 mL/min/kg and oral bioavailability of 30% (Table 1). In our intrinsic clearance studies in cryopreserved hepatocytes, maximum incubation times were 120 min, and thus an upper limit of 790 min was selected as the threshold for how far an estimated half-life could be extrapolated beyond the length of the incubation, assuming 10% bioanalytical variability. This half-life equates to a predicted hepatic clearance of 4.3 mL/min/kg, and thus if the half-life was >790 min, then the predicted hepatic clearance is reported as <4.3 mL/min/kg. The observed in vitro-in vivo disconnect for zaleplon remains unresolved. XK-469 is a low clearance drug in

DMD Fast Forward. Published on October 26, 2011 as DOI: 10.1124/dmd.111.042861
This article has not been copyedited and formatted. The final version may differ from this version.

humans, and this is reflected on our studies, with predicted hepatic clearance values <4.3 mL/min/kg (Table 1). Data confirming that the observed intrinsic clearance in cryopreserved hepatocytes is mediated by AO is reported below.

Intestinal Cytosol. Incubations of each AO substrate with human intestinal cytosol resulted in no measurable metabolism as determined by substrate depletion methodologies (data not shown). Following oral dosing, assuming that fraction absorbed (f_a) is equal to 1 (for top limit estimate), and limited intestinal metabolism (f_g=1), the predicted oral bioavailability using hepatic clearance (Cl_h) estimates and equation 5 for BIBX1382, carbazeran, and zaleplon (dosed orally in the clinic) is ~13%, 15%, and 79%, respectively (Table 1).

Metabolite Profiling. The LC-mass spectrometry data demonstrating the metabolite profiles of AO substrates following incubation with cryopreserved human hepatocytes is shown in Figure 2. For each substrate, the AO-generated metabolite was most predominant. The metabolites generated by aldehyde oxidase for the tested AO substrates in these studies have previously been characterized and reported, with the exception of BIBX1382. Thus, this is the first reported characterization of the AO-mediated metabolism of BIBX1382, where in vitro generated metabolite has been demonstrated as being produced by aldehyde oxidase, matching that of the synthetically prepared metabolite (BIBU1476). Since authentic standard metabolites of the other tested AO substrates were not acquired, a thorough characterization was performed, including incubation in the presence of ~50% $H_2{}^{18}O$ (Figure 4 A-F) in effort to confirm oxidation by molybdenum hydroxylases and not cytochrome P450. Theoretically, the maximal % incorporation of ^{18}O would be 48.5% (incubations conducted in 50/50 mixtures of $H_2{}^{16}O$ and $H_2{}^{18}O$, and $H_2{}^{18}O$ of 97% purity). In addition, MS/MS fragmentation using high resolution mass spectrometry was acquired for each metabolite of interest (supplemental information).

DMD Fast Forward. Published on October 26, 2011 as DOI: 10.1124/dmd.111.042861
This article has not been copyedited and formatted. The final version may differ from this version.

BIBX1382. Figure 3A shows the LC-MS extracted ion chromatogram (XIC) of the hepatocyte generated metabolite of BIBX1382 (*m/z* 404), with the retention time (10.7 min) matching that of the synthetically prepared authentic standard metabolite, BIBU1476. The protonated molecular ion of BIBX1382 was observed at $[M+H]^+$ at *m/z* 388.14 with a retention time of 12.5 min. Fragmentation of BIBX1382 produced three predominant fragment ions at *m/z* 357.1028, *m/z* 345.1027, and *m/z* 291.0559, which all correspond to daughter ions following fragmentation of the methyl-piperidine moiety (Figure 3B). For the predominant oxidized metabolite of BIBX1382, which had a retention time of 10.7 min and produced a protonated molecular ion at $[M+H]^+$ at *m/z* 404.14 (BIBU1476), each of the aforementioned fragment ions shifted 16 Da to *m/z* 373.0976, *m/z* 361.0978, and *m/z* 307.0508, respectively (Figure 3B). In addition, the fragmentation pattern of the metabolically generated oxidative metabolite of BIBX1382 was consistent with the synthetically prepared standard BIBU1476 (data not shown). Incorporation of ^{18}O into the product metabolite was observed following hepatocyte incubations, as evidenced by the presence of the molecular ion at *m/z* 406.1432 (68% relative abundance), which is 2 mass units higher than the metabolite molecular ion at *m/z* 404.1398 (Figure 4A). Incorporation of ^{18}O was roughly 33% (48.5% x 0.68). The resolution of the Orbitrap was increased to 100,000 to derive molecular formulas and distinguish the mass difference between the ^{37}Cl isotope and the ^{18}O isotope and ensure accuracy in the incorporation calculation (Supplemental Figure 1).

Carbazeran. The protonated molecular ion of carbazeran was observed at $[M+H]^+$ at *m/z* 361 with a retention time of 10.9 min. Fragmentation of carbazeran produced a predominant fragment ion at *m/z* 272.1395, corresponding to loss of the ethylcarbamate moiety (-89 Da) (Supplemental Figure 2). The known predominant oxidized metabolite of carbazeran

DMD Fast Forward. Published on October 26, 2011 as DOI: 10.1124/dmd.111.042861
This article has not been copyedited and formatted. The final version may differ from this version.

(phthalazinone) had a retention time of 13.9 min and produced a protonated molecular ion at $[M+H]^+$ at *m/z* 377. Fragmentation of this oxidative metabolite yielded a predominant fragment ion at *m/z* 288.1347, 16 Da higher than the key fragment observed in the parent spectrum. Incorporation of ^{18}O into the phthalazinone metabolite of carbazeran following incubation in hepatocytes was apparent (~47.5% incorporation), with a characteristic isotope pattern showing molecular ions at *m/z* 377.1817 (+16 Da) and 379.1858 (+18 Da) at roughly equivalent abundances (Figure 4B).

O^6-Benzylguanine. The protonated molecular ion of O^6-benzylguanine was observed at $[M+H]^+$ at *m/z* 242 with a retention time of 10.5 min. Fragmentation of O^6-benzylguanine generated a product ion at *m/z* 225.0772, corresponding to loss of the amino moiety (-17 Da) (Supplemental Figure 3). A second diagnostic fragment ion was observed at *m/z* 91.0539, corresponding to the remaining methyl-benzene moiety. The oxidized metabolite of O^6-benzylguanine (8-oxo benzylguanine) had a retention time of 12.5 min and produced a protonated molecular ion at $[M+H]^+$ at *m/z* 258, and upon fragmentation yielded a fragment ion *m/z* 241.0722 that was 16 Da higher than what was observed in the parent spectrum. Remaining intact was the fragment ion observed at *m/z* 91.0539. Incorporation of ^{18}O into the 8-oxo metabolite of O^6-benzylguanine following incubation in hepatocytes was observed (~42% incorporation), with a characteristic isotope pattern showing molecular ions at *m/z* 258.0987 (+16 Da) and 260.1028 (+18 Da) (Figure 4C).

Zaleplon. The protonated molecular ion of zaleplon was observed at $[M+H]^+$ at *m/z* 306 with a retention time of 14.5 min. Fragmentation of zaleplon produced three major product ions at *m/z* 264.1248, *m/z* 288.1248, and *m/z* 236.0934, all corresponding to ions generated by fragmentation of the ethylacetamide moiety (Supplemental Figure 4). The oxidized metabolite

DMD Fast Forward. Published on October 26, 2011 as DOI: 10.1124/dmd.111.042861
This article has not been copyedited and formatted. The final version may differ from this version.

of zaleplon (5-oxo zaleplon) had a retention time of 12.7 min and produced a protonated molecular ion at $[M+H]^+$ at *m/z* 322. Upon fragmentation of this metabolite, the three aforementioned fragment ions in the parent spectrum shifted 16 Da to *m/z* 280.1196, *m/z* 304.1197, and *m/z* 252.0884, respectively. Incorporation of ^{18}O into the 5-oxo metabolite of zaleplon following incubation in hepatocytes was observed (~40% incorporation), with a characteristic isotope pattern showing molecular ions at *m/z* 322.1300 (+16 Da) and 324.1343 (+18 Da) (Figure 4D).

XK-469. The protonated molecular ion of XK-469 was observed at $[M+H]^+$ at *m/z* 345 with a retention time of 17.4 min. Fragmentation of XK-469 produced a predominant fragment ion at m/z 299.0585, corresponding to loss of the acid moiety (-46 Da) (Supplemental Figure 5). The oxidized metabolite of XK-469 (3-oxo XK-469) had a retention time of 15.7 min and produced a protonated molecular ion at $[M+H]^+$ at *m/z* 361. Upon fragmentation of this metabolite, a predominant fragment ion was observed at m/z 315.0533, or 16 Da higher than what was observed in the parent spectrum. Incorporation of ^{18}O into the 3-oxo metabolite of XK-469 following incubation in hepatocytes was observed (~50% incorporation), with a characteristic isotope pattern showing molecular ions at *m/z* 361.0590 (+16 Da) and 363.0631 (+18 Da) (Figure 4E). Figure 4F shows the MS/MS spectra of the 1-hydroxy metabolite of midazolam as a negative control. As expected, incorporation of ^{18}O into the 1-hydroxy metabolite was not observed, consistent with a cytochrome P450-mediated oxidative mechanism where the source of oxygen in product comes from molecular oxygen.

Phenotyping Using Hydralazine. Hydralazine is a known inhibitor of AO, and thus was used in these studies for phenotyping to confirm that the observed metabolic activity in cryopreserved hepatocytes was predominantly mediated by AO. Unfortunately, the metabolic turnover of both

DMD Fast Forward. Published on October 26, 2011 as DOI: 10.1124/dmd.111.042861
This article has not been copyedited and formatted. The final version may differ from this version.

zaleplon and XK-469 was too low in our in vitro system to enable this conclusion when co-incubated with hydralazine. However, upon co-incubation of BIBX1382, carbazeran, and O^6-benzylguanine with hydralazine (50 μM), metabolic clearance was substantially attenuated (Figure 5). Predicted hepatic clearance (Cl_h) values for O^6-benzylguanine, carbazeran, and BIBX1382 was reduced from 12.4, 17.2, and 18.2 mL/min/kg to <4.3, <4.3, and 7 mL/min/kg, respectively, when co-incubated with hydralazine. Meanwhile, when the cytochrome P450 substrate propranolol was incubated in the presence of hydralazine, negligible inhibition of metabolism was observed (data not shown).

DMD Fast Forward. Published on October 26, 2011 as DOI: 10.1124/dmd.111.042861
This article has not been copyedited and formatted. The final version may differ from this version.

Discussion

Aldehyde oxidase (AO) is a cytosolic drug-metabolizing enzyme that has recently been highlighted as having relevance to drug discovery and development (Pryde et al., 2010; Garattini and Terao, 2011). The ideal in vitro system for comprehensively evaluating drug metabolism is theoretically hepatocytes, which contain the full complement of drug-metabolizing enzymes, and are readily available from numerous vendors. However, while AO activity has been demonstrated in cryopreserved human hepatocytes (Sahi et al., 2000), an appropriate characterization of quantitative AO activity has not been reported. Thus, a number of probe substrates of AO were selected for investigational studies to evaluate this activity.

BIBX1382 was a drug candidate evaluated in the clinic as an inhibitor of epidermal growth factor receptor (EGFR) for the treatment of cancer (Solca et al., 2004). In human liver microsomes, it was observed that BIBX1382 was relatively stable, and metabolized by CYP2D6 (Dittrich et al. 1999). In addition, in preclinical pharmacokinetic evaluations in rats and mice, oral bioavailability ranged between 50 and 100%. Following oral dosing to human patients, plasma levels were far below that expected to be efficacious (~5% average absolute oral bioavailability), and a previously uncharacterized metabolite was observed in the urine of one patient, that was also circulating in human plasma at high concentrations (Dittrich et al. 1999). Retrospective experiments by Dittrich et al. suggested that BIBX1382 was metabolized by hepatic AO, although details were not reported. In these studies, BIBX1382 was confirmed to be stable in human liver microsomes, but highly unstable in human liver cytosol, with the AO inhibitor raloxifene completely eliminating metabolism (supplemental Figure 6). In addition, we demonstrate that estimated hepatic clearance of BIBX1382 in cryopreserved hepatocytes is high (17.6 to 18.2 mL/min/kg), a clearance that approaches human liver blood flow. The predominant

DMD Fast Forward. Published on October 26, 2011 as DOI: 10.1124/dmd.111.042861
This article has not been copyedited and formatted. The final version may differ from this version.

metabolite following incubation of BIBX1382 in cryopreserved human hepatocytes had a retention time (Figure 3) and MS/MS fragmentation pattern matching that of the authentic standard metabolite, BIBU1476, with oxidation occurring on the pyrimido-pyrimidine core. Incorporation of ^{18}O-oxygen was observed following hepatocyte incubations (Figure 4A), supporting an AO-mediated mechanism. Total clearance of BIBX1382 following intravenous dosing in humans is reported to be high (25-55 mL/min/kg), which exceeds liver blood flow and suggests that the potential exists for either extra-hepatic clearance or some other phenomena such as partitioning into blood cells. However, if the predicted hepatic clearance obtained from cryopreserved hepatocytes (Cl_h = 17.6-18.2 mL/min/kg) was used to estimate oral bioavailability using equations 3 and 5 (assuming f_{abs} and f_g =1), then low oral exposure (12-15% F, Table 1) would have been predicted following first-pass extraction (actual range was 1.8-12.3 %). Meanwhile, no measurable metabolism was observed in human intestinal cytosol, suggesting that AO activity in the gut would play a minor role in impacting oral absorption.

The inotropic agent carbazeran was previously reported to be almost completely cleared pre-systemically in human via 4-hydroxylation to the phthalazinone metabolite by AO (Kaye et al. 1984), while bioavailability in dog was ~68%, with the predominant metabolic pathway being *O*-demethylation (Kaye et al., 1985). Carbazeran demonstrated a similar profile to BIBX1382, with high clearance observed in cryopreserved hepatocytes (~17.5 mL/min/kg). The predominant oxidative metabolite observed following metabolite profiling eluted at 13.9 min and had a protonated molecular ion at $[M+H]^+$ at *m/z* 377 (Figure 2). In addition, incubations in the presence of ^{18}O-water lead to incorporation of ^{18}O as evidenced by a characteristic mass spectral isotope pattern with roughly equivalent abundance of ions at *m/z* 377.1817 and *m/z* 379.1858 (Figure 4B). Similar to BIBX1382, if calculated hepatic clearance from cryopreserved

hepatocytes is used to estimate oral bioavailability, then low oral exposure (~15% F) would be predicted (Table 1). This is a slight under-prediction from what was observed in humans (<5% F), which suggests there may be other mechanisms contributing to low oral exposure of carbazeran (e.g. absorption), or that AO activity in cryopreserved hepatocytes may be modestly impacted during the process of homogenization of liver, harvesting of cells, and cryopreservation. This is currently being investigated in our lab and will be reported in due course. One parameter that has not been included in this analysis is the effect of plasma protein binding on predicted hepatic clearance. In previous studies by Zientek et al. where scaling of in vitro clearance from human liver cytosol and S-9 fraction was evaluated, clearance values were corrected for free fraction. However, as a general rule, the hepatic clearance for high extraction ratio drugs should be primarily driven by liver blood flow, and not fraction unbound to plasma proteins (e.g. $Cl_h=Q_h$). The efficient hepatic extraction of BIBX1382 and carbazeran following oral dose (e.g. ≤5% F) demonstrates this concept.

O^6-Benzylguanine was reported to be rapidly metabolized in human liver cytosol by AO to the O^6-benzyl-8-oxoguanine metabolite (Roy et al., 1995). Subsequently, *O*^{6}-benzylguanine was shown to be converted primarily by metabolism to the 8-oxo metabolite following intravenous administration to cancer patients (Dolan et al., 1998). Total clearance reported following intravenous dosing was 15.6 mL/min/kg. Given that the 8-oxo metabolite was observed in plasma of patients at levels far exceeding the parent drug levels (2.2-fold higher C_{max} and 12- to 29-fold higher AUC), and that urinary excretion of *O*^{6}-benzylguanine only accounted for 3.2% of the administered dose in humans (Dolan et al., 1998), one can assume that the AO-mediated pathway contributes primarily to the observed clearance. When incubated in cryopreserved human hepatocytes, hepatic clearance values ranged from 11.2 to 12.8

DMD Fast Forward. Published on October 26, 2011 as DOI: 10.1124/dmd.111.042861
This article has not been copyedited and formatted. The final version may differ from this version.

mL/min/kg, representing 72-82% of the observed total clearance in humans. Based on these findings, we conclude that roughly quantitative AO activity is apparent in cryopreserved hepatocytes, and that scaling clearance to humans appears reasonable.

One of the more perplexing findings from these studies was that zaleplon, despite demonstrating moderate to high clearance in humans (15.7 mL/min/kg) and 30% oral bioavailability (Rosen et al., 1999), had low intrinsic clearance in hepatocytes (Table 1). Due to the clearance observed with BIBX1382, carbazeran, and O^6-benzylguanine, it is unlikely that the low intrinsic clearance of zaleplon is due to compromised AO activity in the hepatocytes. In addition, the AO-derived metabolite of zaleplon (5-oxo) was clearly observed and characterized in our analyses (Figure 2), with incorporation of ^{18}O (Figure 4D), consistent with previous reports regarding AO-mediated metabolism of zaleplon (Lake et al., 2002). For an unknown reason, the AO-mediated metabolism is not reflected in intrinsic clearance. Saturation of the AO enzyme at only 1 μM is highly unlikely, as the reported K_m for the 5-oxo pathway in human liver cytosol is 124 μM (Renwick et al., 2002). In addition, intestinal metabolism of zaleplon was not observed in our studies. In short, zaleplon was investigated and shown to have high permeability in Caco-2 cells (data not shown), suggesting that access to the hepatocyte was also not likely to be a limitation. Additional studies would have to be performed to understand the lack of correlation with the observed clearance of zaleplon in humans.

XK-469 is an antitumor agent that was reported to be metabolized by AO, with the 3-oxo metabolite being the predominant metabolite in both urine of dosed patients, and in human hepatocytes (Anderson et al., 2005). However, upon dosing in humans, low clearance was observed (Alousi et al., 2007). Results from our studies using cryopreserved hepatocytes were consistent with these reports. We clearly observed an AO-mediated metabolite (Figure 2), with

DMD Fast Forward. Published on October 26, 2011 as DOI: 10.1124/dmd.111.042861
This article has not been copyedited and formatted. The final version may differ from this version.

incorporation of ^{18}O (Figure 4E), but in vitro clearance values were extremely low (<4.3 mL/min/kg). It was somewhat expected that we would not be able to adequately predict the low observed clearance of XK-469, and this points to the fact that additional hepatocyte systems, such as plated hepatocytes, needs to be investigated where longer incubations can be conducted to enable predicting clearance for slowly metabolized drugs, an issue that plagues low-turnover substrates in general.

Reaction phenotyping studies were also conducted in cryopreserved hepatocytes in order to confirm that the observed clearance values were driven primarily by AO. One practical approach would be to co-incubate with a chemical inhibitor of the enzyme of interest. Several inhibitors of AO have been characterized and may be used in vitro, including raloxifene (Obach et al., 2004; Obach, 2004), and menadione (Obach et al., 2004; Sahi et al. 2008). Raloxifene is complicated in that it also is a mechanisms-based inactivator of cytochrome P450 3A4 (Baer et al., 2007), and menadione non-selectively inhibits many cytochrome P450 enzymes (unpublished observations). Hydralazine, an anti-hypertensive agent, has been reported to be an efficient inhibitor of AO, but not of xanthine oxidase (XO) (Johnson et al., 1985), nor the cytochrome P450 enzymes. Thus, this inhibitor was co-incubated (50 μM) in the presence of AO substrate in hepatocytes. Unfortunately, intrinsic clearance values for zaleplon and XK-469 were already too low to decipher a difference when co-incubated with hydralazine, but the observed clearance values for BIBX1382, carbazeran, and O^6-benzylguanine were all substantially attenuated upon co-incubation with hydralazine (Figure 5), corroborating AO as the metabolic enzyme involved in the clearance of these substrates in cryopreserved hepatocytes.

In summary, the two lots of cryopreserved hepatocytes tested appear to maintain roughly quantitative AO activity, as evidenced by chemical inhibition (e.g. hydralazine), ^{18}O-

incoporation studies, and the ability to adequately scale hepatic clearance for known AO substrates. However, given the reports of the potential instability of AO (Duley et al., 1985; Al-Salmy, 2001), a factor that has not been completely resolved, one likely should not assume that all hepatocyte lots from vendors would possess similar quantitative AO activity. Thus, the recommendation would be to characterize each lot of hepatocytes acquired with control AO substrates prior to implementing them into a screening strategy. Data reported here should help provide a benchmark for expected clearance values when using cryopreserved hepatocytes. Future efforts from our lab in this area will include evaluation of additional hepatocyte systems such as plated hepatocytes for AO activity.

Acknowledgements

The authors would like to thank J. Scott Daniels (Vanderbilt Center for Neurosciences Drug Discovery) for helpful comments on data presentation and Matthew Cerny for thoughtful review of our manuscript.

DMD Fast Forward. Published on October 26, 2011 as DOI: 10.1124/dmd.111.042861
This article has not been copyedited and formatted. The final version may differ from this version.

Authorship Contributions

Participated in research design: Hutzler, Albaugh, Yang, Fisher

Conducted experiments: Yang, Albaugh, Fullenwider, Schmenk

Contributed new reagent or analytic tools: n/a

Performed data analysis: Yang, Albaugh, Fullenwider, Schmenk

Wrote or contributed to the writing of the manuscript: Hutzler, Yang, Albaugh

References

Akabane T, Tanaka K, Irie M, Terashita S and Teramura T (2011) Case report of extensive metabolism by aldehyde oxidase in humans: Pharmacokinetics and metabolite profile of FK3453 in rats, dogs, and humans. *Xenobiotica* **41**:372-384.

Al-Salmy HS (2001) Individual variation in hepatic aldehyde oxidase activity. *IUBMB Life* **51**:249-253.

Alousi AM, Boinpally R, Wiegand R, Parchment R, Gadgeel S, Heilbrun LK, Wozniak AJ, DeLuca P and LoRusso PM (2007) A phase 1 trial of XK469: toxicity profile of a selective topoisomerase IIbeta inhibitor. *Invest New Drugs* **25**:147-154.

Anderson LW, Collins JM, Klecker RW, Katki AG, Parchment RE, Boinpally RR, LoRusso PM and Ivy SP (2005) Metabolic profile of XK469 (2(R)-[4-(7-chloro-2-quinoxalinyl)oxyphenoxy]-propionic acid; NSC698215) in patients and in vitro: low potential for active or toxic metabolites or for drug-drug interactions. *Cancer Chemother Pharmacol* **56**:351-357.

Baer BR, Wienkers LC and Rock DA (2007) Time-dependent inactivation of P450 3A4 by raloxifene: identification of Cys239 as the site of apoprotein alkylation. *Chem Res Toxicol* **20**:954-964.

Beedham C, Bruce SE, Critchley DJ, al-Tayib Y and Rance DJ (1987) Species variation in hepatic aldehyde oxidase activity. *Eur J Drug Metab Pharmacokinet* **12**:307-310.

Beedham C (1987) Molybdenum hydroxylases: biological distribution and substrate-inhibitor specificity. *Prog Med Chem* **24**:85-127.

Diamond S, Boer J, Maduskuie TP, Jr., Falahatpisheh N, Li Y and Yeleswaram S (2010) Species-specific metabolism of SGX523 by aldehyde oxidase and the toxicological implications. *Drug Metab Dispos* **38**:1277-1285.

Dittrich C, Greim G, Borner M, Weigang-Kohler K, Huisman H, Amelsberg A, Ehret A, Wanders J, Hanauske A and Fumoleau P (2002) Phase I and pharmacokinetic study of BIBX 1382 BS, an epidermal growth factor receptor (EGFR) inhibitor, given in a continuous daily oral administration. *Eur J Cancer* **38**:1072-1080.

Dolan ME, Roy SK, Fasanmade AA, Paras PR, Schilsky RL and Ratain MJ (1998) *O*6-benzylguanine in humans: metabolic, pharmacokinetic, and pharmacodynamic findings. *J Clin Oncol* **16**:1803-1810.

Duley JA, Harris O and Holmes RS (1985) Analysis of human alcohol- and aldehyde-metabolizing isozymes by electrophoresis and isoelectric focusing. *Alcohol Clin Exp Res* **9**:263-271.

Garattini E, Fratelli M and Terao M (2008) Mammalian aldehyde oxidases: genetics, evolution and biochemistry. *Cell Mol Life Sci* **65**:1019-1048.

Garattini E and Terao M (2011) Increasing recognition of the importance of aldehyde oxidase in drug development and discovery. *Drug Metab Rev*.

Houston JB (1994) Utility of in vitro drug metabolism data in predicting in vivo metabolic clearance. *Biochem Pharmacol* **47**:1469-1479.

Hutzler JM, Linder CD, Melton RJ, Vincent J and Daniels JS (2010) In vitro-in vivo correlation and translation to the clinical outcome for CJ-13,610, a novel inhibitor of 5-lipoxygenase. *Drug Metab Dispos* **38**:1113-1121.

Johnson C, Stubley-Beedham C and Stell JG (1985) Hydralazine: a potent inhibitor of aldehyde oxidase activity in vitro and in vivo. *Biochem Pharmacol* **34**:4251-4256.

Kaye B, Offerman JL, Reid JL, Elliott HL and Hillis WS (1984) A species difference in the presystemic metabolism of carbazeran in dog and man. *Xenobiotica* **14**:935-945.

Kaye B, Rance DJ and Waring L (1985) Oxidative metabolism of carbazeran in vitro by liver cytosol of baboon and man. *Xenobiotica* **15**:237-242.

Kitamura S, Sugihara K and Ohta S (2006) Drug-metabolizing ability of molybdenum hydroxylases. *Drug Metab Pharmacokinet* **21**:83-98.

Lake BG, Ball SE, Kao J, Renwick AB, Price RJ and Scatina JA (2002) Metabolism of zaleplon by human liver: evidence for involvement of aldehyde oxidase. *Xenobiotica* **32**:835-847.

Obach RS, Baxter JG, Liston TE, Silber BM, Jones BC, MacIntyre F, Rance DJ and Wastall P (1997) The prediction of human pharmacokinetic parameters from preclinical and in vitro metabolism data. *J Pharmacol Exp Ther* **283**:46-58.

Obach RS (2000) Metabolism of ezlopitant, a nonpeptidic substance P receptor antagonist, in liver microsomes: enzyme kinetics, cytochrome P450 isoform identity, and in vitro-in vivo correlation. *Drug Metab Dispos* **28**:1069-1076.

Obach RS, Huynh P, Allen MC and Beedham C (2004) Human liver aldehyde oxidase: inhibition by 239 drugs. *J Clin Pharmacol* **44**:7-19.

Obach RS (2004) Potent inhibition of human liver aldehyde oxidase by raloxifene. *Drug Metab Dispos* **32**:89-97.

Pryde DC, Dalvie D, Hu Q, Jones P, Obach RS and Tran TD (2010) Aldehyde oxidase: an enzyme of emerging importance in drug discovery. *J Med Chem* **53**:8441-8460.

Renwick AB, Ball SE, Tredger JM, Price RJ, Walters DG, Kao J, Scatina JA and Lake BG (2002) Inhibition of zaleplon metabolism by cimetidine in the human liver: in vitro studies with subcellular fractions and precision-cut liver slices. *Xenobiotica* **32**:849-862.

Rosen AS, Fournie P, Darwish M, Danjou P and Troy SM (1999) Zaleplon pharmacokinetics and absolute bioavailability. *Biopharm Drug Dispos* **20**:171-175.

Roy SK, Korzekwa KR, Gonzalez FJ, Moschel RC and Dolan ME (1995) Human liver oxidative metabolism of O^6-benzylguanine. *Biochem Pharmacol* **50**:1385-1389.

Sahi J, Khan KK and Black CB (2008) Aldehyde oxidase activity and inhibition in hepatocytes and cytosolic fractions from mouse, rat, monkey and human. *Drug Metab Lett* **2**:176-183.

Solca FF, Baum A, Langkopf E, Dahmann G, Heider KH, Himmelsbach F and van Meel JC (2004) Inhibition of epidermal growth factor receptor activity by two pyrimidopyrimidine derivatives. *J Pharmacol Exp Ther* **311**:502-509.

Zhang X, Liu HH, Weller P, Zheng M, Tao W, Wang J, Liao G, Monshouwer M and Peltz G (2011) In silico and in vitro pharmacogenetics: aldehyde oxidase rapidly metabolizes a p38 kinase inhibitor. *Pharmacogenomics J* **11**:15-24.

Zientek M, Jiang Y, Youdim K and Obach RS (2010) In vitro-in vivo correlation for intrinsic clearance for drugs metabolized by human aldehyde oxidase. *Drug Metab Dispos* **38**:1322-1327.

Footnotes

Reprint requests to:

Dr. J. Matthew Hutzler

Boehringer-Ingelheim Pharmaceuticals Inc., Translational Research (DMPK)

175 Briar Ridge Road, R&D 10578, Ridgefield, CT 06877

Email: Matt.Hutzler@Boehringer-Ingelheim.com

Legends for Figures

Figure 1. Structures of aldehyde oxidase substrates. Arrows indicate the major site of metabolism.

Figure 2. Representative LC-mass spectrometry extracted ion chromatograms (XIC) of aldehyde oxidase-mediated metabolites following incubation of 10 μM substrate in cryopreserved human hepatocytes (Lot OOO).

Figure 3. (A) Extracted ion chromatogram (XIC) showing the metabolite of BIBX1382 generated following incubation in cyropreserved human hepatocytes matching that of the authentic standard (BIBU1476). (B) Spectra of product ions obtained by mass fragmentation of BIBX1382 at *m/z* 388 (top panel) and the aldehyde oxidase-mediated metabolite BIBU1476 at *m/z* 404 (bottom panel).

Figure 4. High resolution mass spectra of aldehyde oxidase metabolites generated in cyropreserved human hepatocytes following incubation in 48.5% $H_2{}^{18}O$ with (A) BIBX1382, (B) carbazeran, (C) O^6-benzylguanine, (D) zaleplon, (E) XK-469, and (F) midazolam (negative control) demonstrating characteristic isotope pattern following incorporation of oxygen from water into the product metabolites. Inset figures demonstrate spectra from incubations lacking ^{18}O-water.

Figure 5. Metabolic stability of AO substrates O^6-benzylguanine (circles), carbazeran (triangles), and BIBX1382 (squares) in human cryopreserved hepatocytes (lot HuE104) in absence (closed symbols) and in presence of (open symbols) the AO inhibitor hydralazine (50 μM). Predicted hepatic clearance (Cl_h) values for O^6-benzylguanine, carbazeran, and BIBX1382 was attenuated from 12.4, 17.2, and 18.2 mL/min/kg to <4.3, <4.3, and 7 mL/min/kg, respectively, when co-incubated with hydralazine.

Table 1. Summary of Predicted Hepatic Clearance of Aldehyde Oxidase Substrates In Cryopreserved Human Hepatocytes Compared to Reported Human Pharmacokinetic Properties.

Hepatic clearance estimates (mL/min/kg) were calculated as described in *Materials and Methods.* Data are presented as mean (standard deviation) from n=4 replicates.

Substrate	Predicted Hepatic Clearance (mL/min/kg)[a]	Predicted Hepatic Clearance (mL/min/kg)[b]	E_h [c]	Predicted Oral Bioavailability [d]	Human Total Clearance (mL/min/kg)	Human Oral Bioavailability (%F)	Reference
BIBX1382	17.6 (0.2)	18.2 (0.2)	85-88	12-15	25-55	2-12	Dittrich et al. 2002
Carbazeran	17.8 (0.1)	17.3 (0.6)	84-86	14-16	38	<5	Kaye et al. 1984
O^6-Benzylguanine	11.2 (0.2)	12.8 (0.2)	54-62	-	15.6	-	Dolan eta al. 1998
Zaleplon	<4.3	<4.3	<21	>79	15.7	30	Rosen et al. 1999
XK-469	<4.3	<4.3	<21	-	<1	-	Alousi et al. 2007

[a] Celsis/In Vitro Technologies (Lot OOO)
[b] Life Technologies (Lot HuE104)
[c] Calculated using Equation 3 using range of hepatic clearance values observed in cryopreserved hepatocytes
[d] Calculated using Equation 5

Figure 1

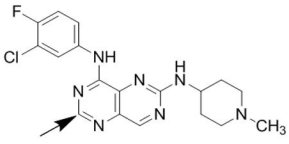

BIBX1382

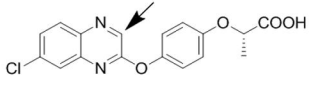

XK-469

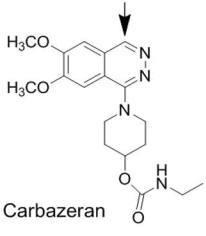

Carbazeran

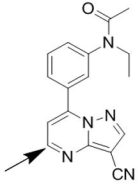

Zaleplon

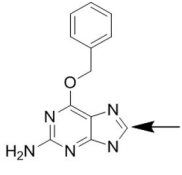

O^6-Benzylguanine

Figure 2

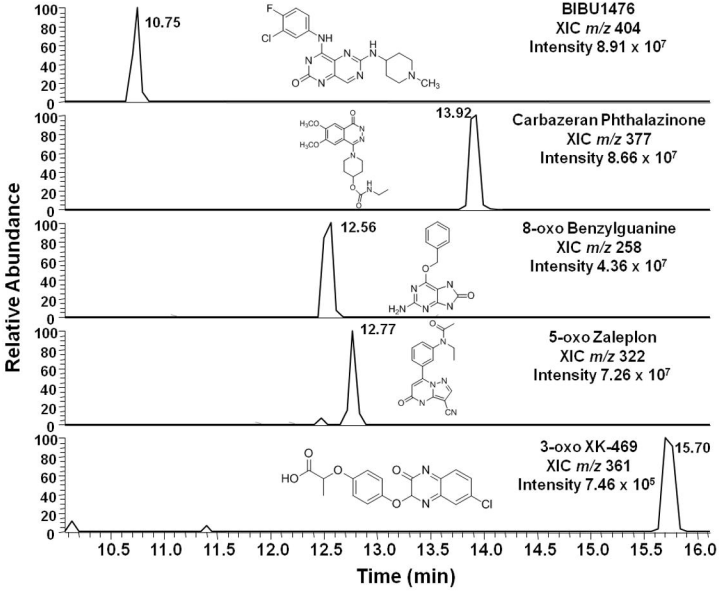
Relative Abundance
Time (min)
10.75
BIBU1476
XIC m/z 404
Intensity 8.91 x 10^7
13.92
Carbazeran Phthalazinone
XIC m/z 377
Intensity 8.66 x 10^7
12.56
8-oxo Benzylguanine
XIC m/z 258
Intensity 4.36 x 10^7
12.77
5-oxo Zaleplon
XIC m/z 322
Intensity 7.26 x 10^7
15.70
3-oxo XK-469
XIC m/z 361
Intensity 7.46 x 10^5

Figure 3

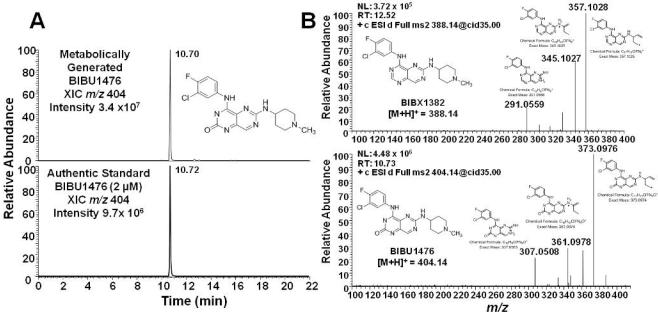
A
Metabolically Generated BIBU1476 XIC m/z 404 Intensity 3.4 x10^7
10.70
Authentic Standard BIBU1476 (2 µM) XIC m/z 404 Intensity 9.7x 10^6
10.72
Relative Abundance
Time (min)
B
NL: 3.72 x 10^5
RT: 12.52
+ c ESI d Full ms2 388.14@cid35.00
BIBX1382
[M+H]+ = 388.14
357.1028
345.1027
291.0559
373.0976
NL: 4.48 x 10^6
RT: 10.73
+ c ESI d Full ms2 404.14@cid35.00
BIBU1476
[M+H]+ = 404.14
361.0978
307.0508
Relative Abundance
m/z

Figure 4

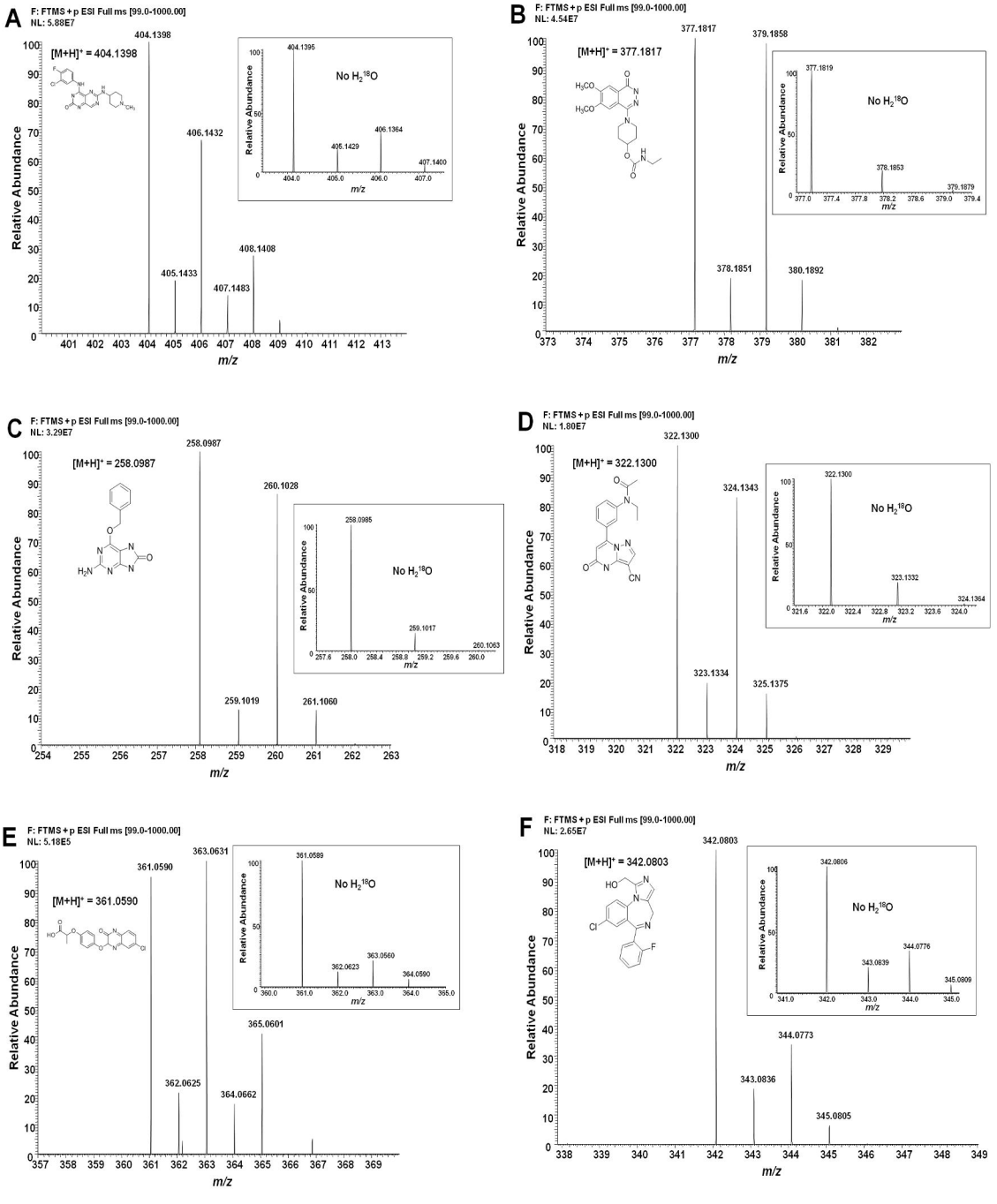
A
F: FTMS + p ESI Full ms [99.0-1000.00]
NL: 5.88E7
[M+H]+ = 404.1398
No H2 18O
B
F: FTMS + p ESI Full ms [99.0-1000.00]
NL: 4.54E7
[M+H]+ = 377.1817
No H2 18O
C
F: FTMS + p ESI Full ms [99.0-1000.00]
NL: 3.29E7
[M+H]+ = 258.0987
No H2 18O
D
F: FTMS + p ESI Full ms [99.0-1000.00]
NL: 1.80E7
[M+H]+ = 322.1300
No H2 18O
E
F: FTMS + p ESI Full ms [99.0-1000.00]
NL: 5.18E5
[M+H]+ = 361.0590
No H2 18O
F
F: FTMS + p ESI Full ms [99.0-1000.00]
NL: 2.65E7
[M+H]+ = 342.0803
No H2 18O
Relative Abundance
m/z

Figure 5

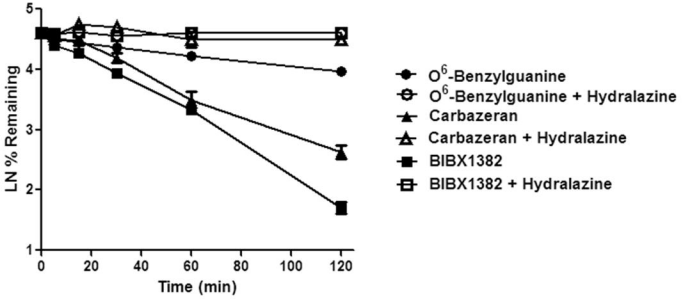
LN % Remaining
5
4
3
2
1
0
20
40
60
80
100
120
Time (min)
O6-Benzylguanine
O6-Benzylguanine + Hydralazine
Carbazeran
Carbazeran + Hydralazine
BIBX1382
BIBX1382 + Hydralazine